

Phase Transition and Elasticity of Gallium Arsenide under Pressure

Emre Güler*, Melek Güler

Department of Physics, Hitit University, 19030, Corum, Turkey

Received: February 10, 2014; Revised: July 8, 2014

Geometry optimization calculations were performed for some structural, elastic and mechanical properties of gallium arsenide (GaAs) under pressures up to 25 GPa. In contrast to previous works, a recent Stillinger-Weber type potential was used for the first time to elaborate the pressure dependence aspects of GaAs. B3→B1 phase transition pressure was determined as 17 GPa. Pressure dependence of density, typical cubic elastic constants, bulk, shear, and Young moduli, Poisson ratio, elastic velocities, anisotropy parameter, Kleinman parameter, elastic anisotropy degree, and stability conditions of GaAs were also evaluated. Overall, our results are satisfactory and can be helpful for future investigations of GaAs under pressure.

Keywords: GaAs, elasticity, elastic constants, pressure, phase transition

1. Introduction

Elastic properties of materials under pressures provide better understanding of some physical knowledge comprising the interatomic forces, mechanical features, phase transitions and so forth. However, elastic property measurements under pressure are usually very difficult and the lack of experimental data can be compensated by computational methods¹.

GaAs is a very well-known III-V semiconductor and has many unique properties, which makes it important for rapidly developing optoelectronic technology. The most remarkable uses of GaAs cover photovoltaics, heterostructures, semiconductor lasers, light-emitting diodes and solar cells²⁻¹⁰.

GaAs has several phases and crystallizes in the cubic zinc blend phase (B3) at ambient conditions. Under pressure, zinc blend phase can transform to sodium chloride phase (B1)^[11]. It is worth to note here that, other observed high-pressure phases of GaAs (i.e. orthorhombic Imm2 phase above 25 GPa and hexagonal cinnabar phase between 60GPa and 80 GPa)^[2-11] are not the focus of our study.

Apart from many experimental efforts^{4,10}, Rino et al.¹² calculated phase transition pressure (P_T) as 22 GPa for GaAs with molecular dynamics in 2002. Later, Yu et al.⁷ stated P_T as 16.3 GPa by density functional theory. Afterwards, Varshney and his collaborators conferred P_T as 17 GPa in their pure theoretical paper¹¹. Yu et al., Al-Douri and Reshak, Bueno et al., Christensen, Varshney et al. and Rino et al.⁷⁻¹² have extreme motivation on P_T , cubic elastic constants and bulk modulus. However, pressure dependence of young modulus, shear modulus, elastic wave velocities, Poisson ratio, elastic anisotropy, Kleinman parameter, anisotropy degree are still lacking for GaAs except the analysis of Varshney et al.¹¹. So, our objective is to elaborate these parameters by geometry optimization calculations. In contrast to previous methods and applied potentials and to the best of our knowledge, this is the first survey reporting

the application of a recent and modified Stillinger-Weber type potential to GaAs under pressure.

The rest of the paper is organized as follows. After this introduction, a brief outline for geometry optimization and computational details are given in Section 2. Our calculations results are presented and discussed in Section 3. We then summarize and conclude in Section 4.

2. Computational Details

Geometry optimization is an efficient and convenient method for both molecular dynamics and density functional theory to get a stable configuration for a molecule or periodic system through fast and inexpensive energy computations. An optimization procedure involves the repeated sampling of the potential energy surface until the potential energy reaches a minimum where all forces on all atoms are zero. All herein done geometry optimization calculations were performed with General Utility Lattice Program (GULP) code 4.0.^[13,14] during the present work. GULP code allows wide-range property calculations for 3D periodic solids, 2D surfaces, and gas phase clusters by employing two-body, three-body, four-body, six-body, and many body (EAM) potentials^{15,16} depending on the demands of research. Since Stillinger-Weber type potentials provide reliable results especially for semiconductors, we employed a recent and modified Stillinger-Weber type potential¹⁷ to research for GaAs. The lattice constant for GaAs was set as $a_0 = 5.66$ Å which is slightly higher than the experimental lattice constant $a_{exp} = 5.65$ Å. Other details of applied Stillinger-Weber type potential and its modified parameterization procedure can be also found in Han and Bester¹⁷. It is also possible to optimize related structures at constant pressures (includes all internal and cell variables) and constant volume (unit cell remains frozen) with GULP^[1,13-16,18]. Constant pressure optimization was performed for GaAs in our survey. The geometry of cells was optimized by the Newton-Raphson method based on the Hessian matrix

*e-mail: eguler71@gmail.com

calculated from the second derivatives and Hessian matrix was recursively updated during optimization by using the BFGS^[1,13-16,18] algorithm. After setting the preconditions for the B3 crystal structure of GaAs, we adopted multiple runs at zero Kelvin temperature and checked the pressure ranges starting from 0 GPa up to 25 GPa.

3. Results and Discussion

B3→B1 phase transition pressure of GaAs was determined from P-V plot as seen in Figure 1. The volume of GaAs has a sudden decrease at 17 GPa. This abrupt decrease in volume originates from the structural phase change associated with the B3→B1 phase transition. The obtained value for P_T (17 GPa) not only agrees well with experimental value of 16.6 GPa, but also in the range of former theoretical data (See Table 1).

As pointed out by Douri and Ressaq, III-V compounds are low-density materials which can they display structural phase transitions to a higher density phase under pressure⁸. In fact, as clear from Figure 2, density of GaAs increases with the increasing pressure between 0 GPa and 25 GPa and our results confirms the findings of Al-Douri and Reshak⁸.

Typical cubic elastic constants (C_{11} , C_{12} and C_{44}) define the mechanical hardness and necessary for specifying the stability of the material. These constants derived from the total energy calculations represent the single crystal elastic properties. On the other hand, Voigt-Reuss-Hill approach is

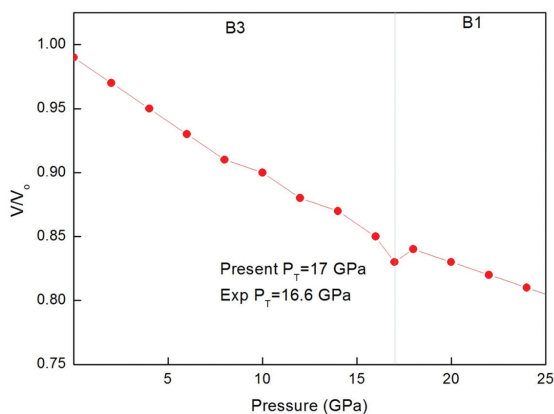


Figure 1. P-V plot of GaAs up to 25 GPa.

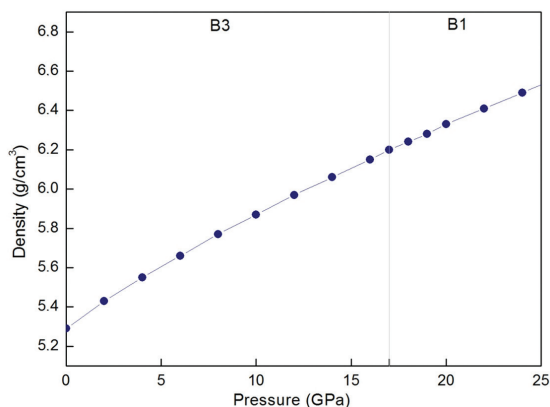


Figure 2. Pressure dependence of density in GaAs up to 25 GPa.

a confident scheme for elastic constants of polycrystalline materials¹⁹. To get the correct values of elastic constants and other connected parameters of GaAs, we considered the Voigt-Reuss-Hill values during calculations. Table 1 lists obtained elastic constants with existing experimental and theoretical data for the sake of comparison. Our results are both consistent with experiments and prior theoretical data^{6,11-14}. Further, elastic constants show a smooth increment with increasing pressure in both B3 and B1 phases for the entire pressure range as in Figure 3. Besides, increment of C_{11} is higher than C_{12} and C_{44} . Physically, C_{11} portrays the longitudinal elastic behavior whereas C_{12} and C_{44} explain the off diagonal and shear elastic characteristic of cubic crystals because of shearing, respectively. So, a longitudinal strain produces a change in volume without a change in shape. This volume change is related to pressure, thus reflects a larger change in C_{11} . Contrarily, a transverse strain or shearing causes a change in shape without a change in volume. So, C_{12} and C_{44} are less sensitive to pressure than C_{11} .

According to Born structural stability, elastic constants must satisfy the conditions: $C_{11} - C_{12} > 0$, $C_{11} > 0$, $C_{44} > 0$, $C_{11} + 2C_{12} > 0$, and cubic stability e.g. $C_{12} < B < C_{11}$ ^[20]. As another result, present C_{11} , C_{12} , and C_{44} values well support both structural and cubic stability conditions for GaAs.

Bulk modulus (B) offers much information about bonding strength of materials and it is a measure of resistance to external deformation^{21,22}. Figure 4 displays the pressure behavior of three elastic moduli (B , G , and E) of GaAs for entire pressure scale. By the way, shear modulus, (G) defines the resistance to shape change caused by a shearing force^{23,24}. Young modulus (E) is the resistance to uniaxial tensions and gives the stiffness degree i.e., the higher the value of E , the stiffer is the material^{25,26}. From the prevalent physical equation of bulk modulus ($B = \Delta P/\Delta V$) one can expect an increment for B due its direct proportion to applied pressure. Thus, bulk modulus of GaAs show a linear increment in both B3 and B1 phases as expected in Figure 4. As well, B3 structure has a larger stiffness than B1 structure because of its higher young modulus values than B1. Numerical values of B , G , and E are further compared in Table 1. The calculated value of B is satisfactory with experiments, whereas present results of both G and E moduli underestimate the experimental data.

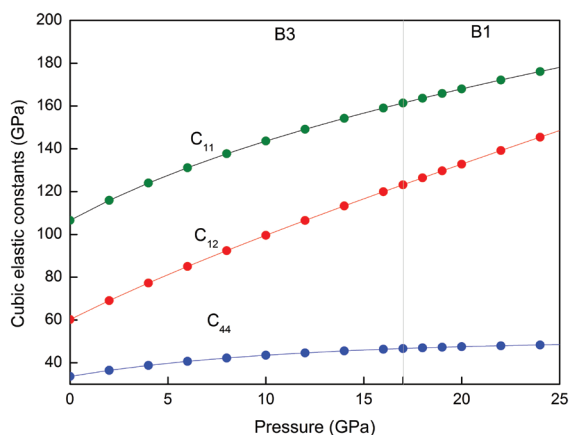


Figure 3. Typical cubic elastic constants C_{11} , C_{12} and C_{44} of GaAs under pressure.

Since ductility and brittleness play a key role during materials manufacturing, we also appraised the ductile (brittle) nature of GaAs under pressure. The adjectives brittle and ductile stand for the two separate mechanical behaviors of solids when they subjected to stress. Usually, brittle materials are not deformable or less deformable before fracture. Unlike brittle materials, ductile materials are deformable a lot before fracture. At this point, Pugh ratio is a determinative limit for ductile (brittle) behavior²⁷ and has a common use in literature. If B/G ratio is about 1.75 and higher, the material is ductile, otherwise the material becomes brittle. Another reliable approach is Cauchy pressure, which is defined as $C_p = C_{12} - C_{44}$. The negative (positive) values of the Cauchy pressure show the brittle (ductile) nature of the compounds²⁸. So, we cross-checked the obtained results with these norms.

Figure 5 is a plot of the Pugh B/G ratio region of the GaAs up to 25 GPa. In Figure 5, Pugh ratio analysis proves the ductile nature of GaAs under pressure. After a cross-check Cauchy pressure values corroborates the same behavior. As another result, all values of the B/G are higher than 1.75 and increase with pressure, which mean that pressure can improve ductility.

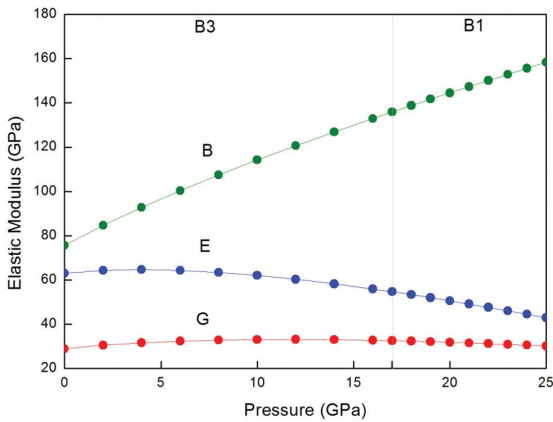


Figure 4. Pressure dependence of elastic moduli B, E, and G in GaAs.

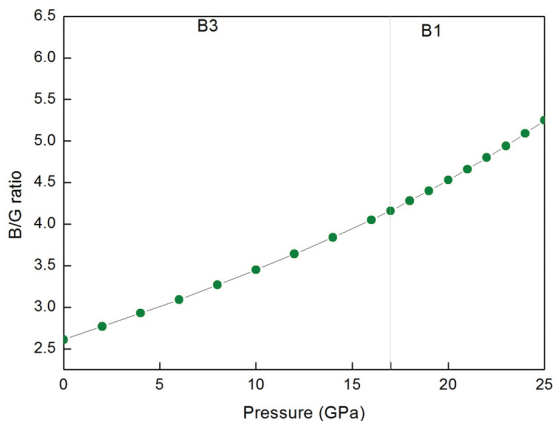


Figure 5. B/G ratio versus pressure for GaAs.

Poisson ratio (ν) is the ratio between the transverse strain (e_t) and longitudinal strain (e_l) in the elastic loading direction. It delivers detailed knowledge about the bonding force behavior in solids^{15,29}. $\nu = 0.25$ and $\nu = 0.5$ values are the lower limit and upper limit for central force solids, respectively. Poisson ratio begins with 0.36 and increases with applied pressure as in Figure 6. This result suggests that interatomic forces in the GaAs are mainly central forces. Moreover, 0.36 value for ν is close to experiments (See Table 1).

In solids, vibrational excitation starts from low-temperature acoustic modes. Being dependent on this case, two typical elastic waves namely the longitudinal wave (V_L) and shear wave (V_s) arise¹⁵. V_L has a uniform increment trend with the increasing pressure in B3 and B1 phases in Figure 7 whereas V_s is increasing in the B3 phase and decreasing in the B1 phase. The current data of V_L and V_s well satisfy the experiments as can be seen from Table 1.

Kleinman parameter (ζ) for cubic materials describes the relative ease of bond bending to the bond stretching. Minimizing bond bending leads $\zeta = 0$ and minimizing bond stretching leads to $\zeta = 1$. In addition, Kleinman parameter links to elastic constants as $\zeta = C_{11} + 8C_{12} / 7C_{11} + 2C_{12}$ ^[30]. Figure 8 displays the Kleinman parameter upon the pressure

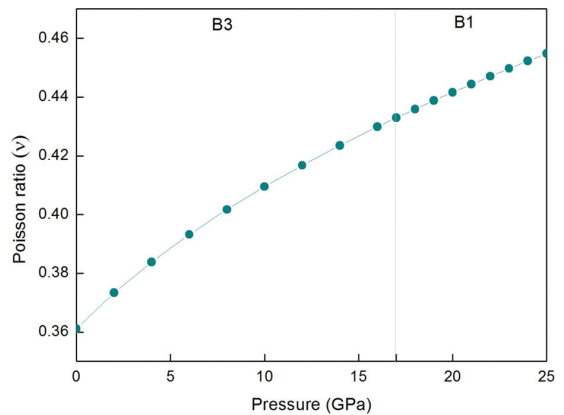


Figure 6. Poisson ratio behavior under pressure for GaAs.

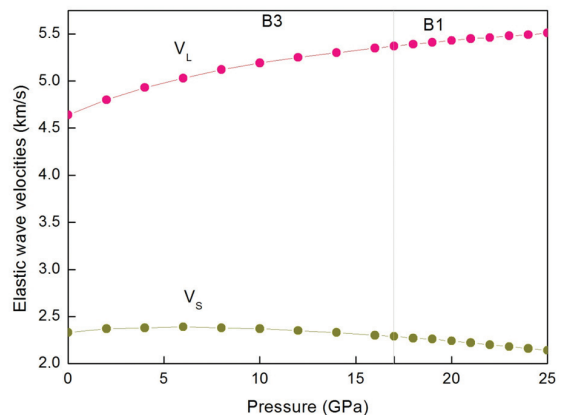
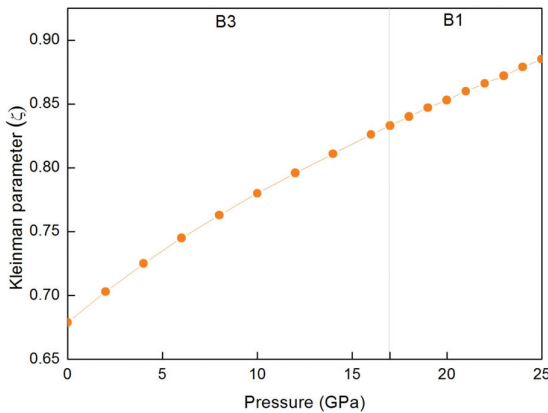


Figure 7. Pressure dependence of elastic wave velocities of (V_L and V_s) GaAs up to 25 GPa.

Table 1. Comparing some structural, elastic and mechanical parameters of GaAs with previous and present results.

Parameter	Present	Experiments	Other theoretical results
a (Å)	5.66	5.65 ⁽³³⁾	5.56 ⁽¹⁷⁾ , 5.64 ⁽⁷⁾
d (g/cm ³)	5.29	5.32 ⁽³⁴⁾	
P_T (GPa)	17	16.6 ⁽¹⁰⁾	10.5 ⁽³³⁾ -17 ⁽¹¹⁾
C_{11} (GPa)	106.5	106.5 ⁽⁴⁾	122.3-147.6 ⁽¹¹⁾
C_{12} (GPa)	60.2	53.3 ⁽⁴⁾	40.6-119 ⁽¹¹⁾
C_{44} (GPa)	33.6	60.2 ⁽⁴⁾	42.4-107 ⁽¹¹⁾
B (GPa)	75.6	75.5 ⁽⁴⁾	70.8-135 ⁽¹¹⁾
G (GPa)	28.9	32.6 ⁽⁴⁾	24.5 ⁽¹¹⁾
E (GPa)	63.0	85.5 ⁽⁴⁾	
ν	0.36	0.31 ⁽³⁴⁾	
V_L (km/s)	4.64	4.73 ⁽⁴⁾	6.89 ⁽¹¹⁾
V_S (km/s)	2.33	3.34 ⁽⁴⁾	3.87 ⁽¹¹⁾
ζ	0.67	0.58 ⁽¹⁷⁾	0.81 ⁽¹¹⁾

**Figure 8.** Behavior of Kleinman parameter under pressure for GaAs.

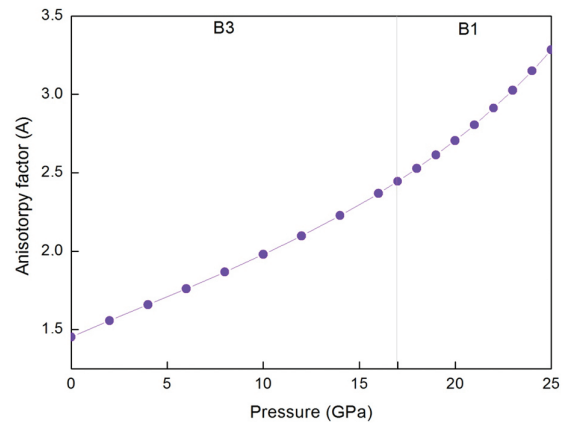
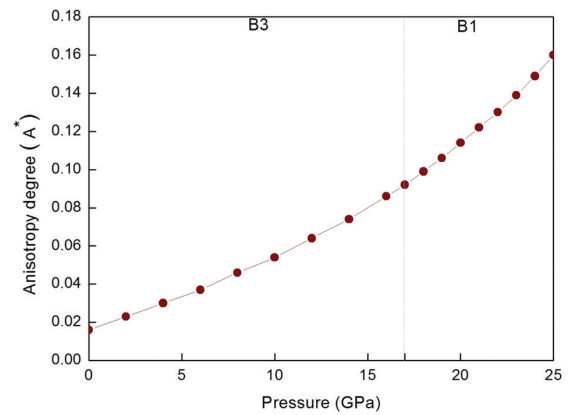
increment. Under pressure, ζ increases with increasing pressure and it is found to be between 0.65 and 0.90. So, present Kleinman value 0.65 is better than those of other reports (See Table 1).

The elastic anisotropy of crystals has an important implication in engineering since it is correlated with the possibility to persuade microcracks in the materials. For that reason, the anisotropy factor $A = 2C_{44} / (C_{11} - C_{12})$ ⁽³¹⁾ has been evaluated for a deeper view on the elastic anisotropy of the GaAs. In the applied pressure range in Figure 9, the obtained anisotropy factors A are not equal to 1, which means the presence of elastic anisotropy in GaAs.

A convenient method of describing the degree of elastic anisotropy for a cubic crystal has been formulated as³²:

$$A^* = \left[3(A-1)^2 \right] / \left[3(A-1)^2 + 25A \right]$$

Degree of elastic anisotropy (A^*) in GaAs shows a monotonous increment as the pressure increases and the increment in B1 structure is higher than B3 structure. It is evident from Figure 10 that GaAs has a profound elastic

**Figure 9.** Anisotropy factor of GaAs versus pressure.**Figure 10.** Degree of anisotropy for GaAs between 0 GPa and 25 GPa.

anisotropy since the degree of elastic anisotropy for B3 structure is smaller than the B1 structure of the GaAs.

In summary, existing results of this survey show a fair agreement with the experiments, especially on the bulk modulus and phase transition pressure as obvious in Table 1. Although current findings slightly underestimate shear modulus and C_{44} of GaAs, our other results are better than those of Varshney et al.¹¹ and fairly agree with experiments and other data.

4. Conclusions

It should be noted that the merit of this work is not only calculating the C_{11} , C_{12} and C_{44} , B , P_T data of GaAs under pressure but also explaining pressure dependence of other important data such as E , G , V_L and V_S , ν , ζ , A and A^* . Application of a recent Stillinger-Weber type potential, which is originally, used to predict phonon and related properties of GaAs¹⁷ well reproduce other mechanical, structural, and elastic features of GaAs under pressure. Finally, our detailed results can be useful for the lack of experimental data and inspire future theoretical works.

References

- Güler E and Güler M. Geometry optimization calculations for the elasticity of gold at high pressure. *Advances in Materials Science and Engineering*. 2013; 2013:1-5. <http://dx.doi.org/10.1155/2013/525673>
- Baaziz H, Charifi Z, Ressaq AH, Hamad B and Al-Douri Y. Structural and electronic properties of GaN x As $1-x$ alloys. *Applied Physics A*. 2012; 106(3):687-696. <http://dx.doi.org/10.1007/s00339-011-6666-8>
- Cui HL, Chen XR, Ji GF and Wei DQ. Structures and Phase Transition of GaAs under Pressure. *Chinese Physics Letters*. 2008; 25(6):2169-2172. <http://dx.doi.org/10.1088/0256-307X/25/6/067>
- Blakemore JS. Semiconducting and other major properties of gallium arsenide. *Journal of Applied Physics*. 1982; 53(10):R123. <http://dx.doi.org/10.1063/1.331665>
- Al-Douri Y. Confirmation of bulk modulus model of III-V compounds under pressure effect using tight-binding method. *Optik: International Journal for Light and Electron Optics*. 2012; 123(11):989-992. <http://dx.doi.org/10.1016/j.ijleo.2011.07.016>
- Al-Douri Y, Reshak AH and Hashim U. Optoelectronic properties of GaAs and AlAs under temperature effect. *Optik: International Journal for Light and Electron Optics*. 2013; 124(15):2128-2130. <http://dx.doi.org/10.1016/j.ijleo.2012.06.063>
- Yu LL, Rong CX, Ru YB and Quan GQ. First-principles calculations for transition phase and thermodynamic properties of GaAs. *Chinese Physics*. 2006; 15(4):802. <http://dx.doi.org/10.1088/1009-1963/15/4/022>
- Al-Douri Y and Reshak AH. Calculated optical properties of GaX (X=P, As, Sb) under hydrostatic pressure. *Applied Physics A*. 2011; 104(4):1159-1167. <http://dx.doi.org/10.1007/s00339-011-6400-6>
- Bueno CF, Machado DHO, Pineiz TF and Scalvi LVA. Photo-Induced conductivity of heterojunction GaAs/Rare-Earth doped SnO₂. *Materials Research*. 2013; 16(4):831-838. <http://dx.doi.org/10.1590/S1516-14392013005000060>
- Christensen NE. Electronic structure calculations for semiconductors under pressure. In: Suski T and Paul W, editors. *High pressure in semiconductor physics I*. New York: Academic Press; 1998.
- Varshney D, Joshi G, Varshney M and Shriya S. Pressure dependent elastic and structural (B₃-B₁) properties of Ga based mononitrides. *Journal of Alloys and Compounds*. 2010; 495(1):23-32. <http://dx.doi.org/10.1016/j.jallcom.2010.01.077>
- Rino JP, Chatterjee A, Ebbsjö I, Kalia RK, Nakano A, Shimojo F et al. Pressure-induced structural transformation in GaAs: a molecular-dynamics study. *Physical Review B*. 2002; 65.
- Gale JD. GULP: a computer program for the symmetry-adapted simulation of solids. *Journal of the Chemical Society, Faraday Transactions*. 1997; 93(4):629-637. <http://dx.doi.org/10.1039/a606455h>
- Gale JD and Rohl AL. The General Utility Lattice Program (GULP). *Molecular Simulation*. 2003; 29(5):291-341. <http://dx.doi.org/10.1080/0892702031000104887>
- Güler M and Güler E. Embedded atom method-based geometry optimization aspects of body-centered cubic metals. *Chinese Physics Letters*. 2013; 30(5):056201. <http://dx.doi.org/10.1088/0256-307X/30/5/056201>
- Gale JD. GULP: capabilities and prospects. *Zeitschrift für Kristallographie: Crystalline Materials*. 2005; 220(5-6):552-554.
- Han P and Bester G. Interatomic potentials for the vibrational properties of III-V semiconductor nanostructures. *Physical Review B*. 2011; 83:174304. <http://dx.doi.org/10.1103/PhysRevB.83.174304>
- Gale JD. *Molecular modeling theory: applications*. In: Timothy CR and Kubicki JD, editors. *The Geosciences*. Washington: Mineralogical Society of America; 2001. cap. 2. p. 37.
- Ponomareva AV, Isaev E, Vekilov YK and Abrikosov I. Site preference and effect of alloying on elastic properties of ternary B 2 NiAl-based alloys. *Physical Review B*. 2012; 85:144117. <http://dx.doi.org/10.1103/PhysRevB.85.144117>
- Güler E and Güler M. A benchmark for some bulk properties of bcc iron. *International Journal of Multiphysics*. 2013; 7(2):95-100. <http://dx.doi.org/10.1260/1750-9548.7.2.95>
- Bensalem S, Chegaar M, Maouche D and Bouhemadou A. Theoretical study of structural, elastic and thermodynamic properties of CZTX (X = S and Se) alloys. *Journal of Alloys and Compounds*. 2014; 589:137-142. <http://dx.doi.org/10.1016/j.jallcom.2013.11.113>
- Guemou M, Abdiche A, Riane R and Khenata R. Ab initio study of the structural, electronic and optical properties of BAs and BN compounds and BN x As $1-x$ alloys. *Physica B: Condensed Matter*. 2014; 436:33-40. <http://dx.doi.org/10.1016/j.physb.2013.11.030>
- Gao X, Jiang Y, Zhou R and Feng J. Stability and elastic properties of Y-C binary compounds investigated by first principles calculations. *Journal of Alloys and Compounds*. 2014; 587:819-826. <http://dx.doi.org/10.1016/j.jallcom.2013.11.005>
- Zhang M, Yan H, Zhao Y and Wei Q. Mechanical properties and atomistic deformation mechanism of spinel-type BeP₂N₄. *Computational Materials Science*. 2014; 83:457-462. <http://dx.doi.org/10.1016/j.commatsci.2013.11.044>
- Wang S, Li JX, Du YL and Cui C. First-principles study on structural, electronic and elastic properties of graphene-like hexagonal Ti₂C monolayer. *Computational Materials Science*. 2014; 83:290-293. <http://dx.doi.org/10.1016/j.commatsci.2013.11.025>
- Feng LP, Li N, Yang MH and Liu ZT. Effect of pressure on elastic, mechanical and electronic properties of WSe₂: a first-principles study. *Materials Research Bulletin*. 2014; 50:503-508. <http://dx.doi.org/10.1016/j.materresbull.2013.11.016>
- Rahmati A, Ghoostani M, Bادهian H and Baizae M. Ab initio study of the structural, elastic, electronic and optical properties of Cu₃N. *Materials Research*. 2014; 17(2):303-310. <http://dx.doi.org/10.1590/S1516-14392014005000039>
- Kanchana V and Ram S. Electronic structure and mechanical properties of Sc₃AC (A = Al, Ga, In, Tl) and Sc₃BN (B = Al, In): Ab-initio study. *Intermetallics*. 2012; 23:39-48. <http://dx.doi.org/10.1016/j.intermet.2011.12.014>
- Greaves GN, Greer AL, Lakes RS and Rouxel T. Poisson's ratio and modern materials. *Nature Materials*. 2011; 10:823-837. PMID:22020006. <http://dx.doi.org/10.1038/nmat3134>
- Ustundag M, Aslan M and Yalcin BG. The first-principles study on physical properties and phase stability of Boron-V (BN, BP, BAs, BSb and BBi) compounds. *Computational Materials Science*. 2014; 81:471-477. <http://dx.doi.org/10.1016/j.commatsci.2013.08.056>
- Maachou A, Aboura H, Amrani B, Khenata R, Bin Omran S and Varshney D. Structural stabilities, elastic and thermodynamic properties of Scandium Chalcogenides via first-principles calculations. *Computational Materials Science*. 2011; 50:3123-3130. <http://dx.doi.org/10.1016/j.commatsci.2011.05.038>
- Bing L, Feng LR, Yong Y and Dong YX. Characterisation of the high-pressure structural transition and elastic properties in boron arsenic. *Chinese Physics B*. 2010; 19(7):076201. <http://dx.doi.org/10.1088/1674-1056/19/7/076201>
- Adachi S. *Properties of Group-IV, II-V and II-VI semiconductors*. England: John Wiley & Sons; 1994.
- Sze SM. *Semiconductor sensors*. New York: John Wiley & Sons; 1994.